Autocatalytic duplex Ni-P/Ni-W-P coatings on AZ 31B magnesium alloy

V. Ezhil Selvi[a *], Purba Chatterji[a], S. Subramanian[b], J.N.Balaraju[a*]

[a]Surface Engineering Division, CSIR National Aerospace Laboratories, Post Bag No. 1779, Bangalore 560017, India
[b]Department of Materials Engineering, Indian Institute of Science, Bangalore 560 012, India

Abstract

Autocatalytic duplex Ni-P/Ni-W-P coatings were deposited on AZ31B magnesium alloy using stabilizer free nickel carbonate bath. Some of the coated specimens were passivated in chromate solution with and without heat treatment. Plain Ni-P coatings were also prepared for comparison. Coatings were characterized for their surface morphology, composition and corrosion resistance. Energy dispersive analysis of X-ray (EDX) showed that the duplex coating contained about 3 wt.% P and 2 wt.% W with balance Ni. Marginal increase in P and W contents were observed on passivated coupons along with Cr (0.18 wt.%) and O (2.8 wt.%) contents. Field emission scanning electron microscopy (FESEM) examination of these coatings surfaces exhibited the nodular morphology. Chromate passivated surfaces showed the presence of uniformly distributed bright Ni particles along with nodules. Potentiodynamic polarization and electrochemical impedance spectroscopy (EIS) studies were carried out in deaerated 0.15 M NaCl solution to find out the corrosion resistance of the coatings. Among the coatings developed, duplex-heat treated-passivated (duplex-HTP) coatings showed lower corrosion current density (i_{corr}) and higher polarization resistance (R_p) indicating the improved corrosion resistance. The charge transfer resistance (R_{ct}) value obtained for the duplex-HTP was about 170 times higher compared to Ni-P coating.

Keywords: Magnesium alloy; Duplex Ni-P/Ni-W-P; Corrosion; EIS

*Corresponding author. Tel.: +91 80 2508 6245; Fax: +91 80 2521 0113
E-mail address: ezhil222@nal.res.in (V. EZHIL SELVI)

*Corresponding author. Tel.: +91 80 2508 6239; Fax: +91 80 2521 0113
E-mail address: jnbalraj@nal.res.in (J. N. BALARAJU)

1. Introduction

Magnesium (Mg) and its alloys are extensively used for various industries such as aerospace, automobile and electronics due to their excellent properties such as low density, high strength and stiffness and electromagnetic shielding [1]. However, the wide spread applications of these alloys were limited due to the undesirable properties such as poor corrosion and wear resistance, poor creep resistance and high chemical reactivity respectively. These alloys are highly susceptible to galvanic corrosion in sea water environment due to high negative potential (-2.37 V vs SHE). The effective way of preventing corrosion is through the formation of a protective coating which acts as the barrier between the corrosive medium and the substrate. Many surface modification methods such as electro/ electroless plating, conversion coating, physical and chemical vapor depositions, thermal spray coating etc., are available to-date to improve the corrosion resistance of Mg alloys [2-5]. Of these methods, the electroless nickel plating has gained considerable importance because of its excellent properties such as high hardness, good wear and corrosion resistance. Properties of the binary electroless nickel coating have been further improved by the addition of third elements such as cobalt, tungsten, tin and copper etc. It has been reported that the addition of tungsten as the third element in the Ni-P improves the properties such as hardness, wear and corrosion resistance, thermal stability and electrical resistance [6, 7].

Magnesium alloys are categorized as a “difficult to plate metal”, because of its high reactivity in the aqueous solution. It reacts vigorously with atmospheric oxygen and water, resulting in the formation of the porous oxide/ hydroxide film which does not provide any protection in corrosive environment. Further, the presence of this oxide film prevents the formation of good adhesive bond between the coating and the substrate. The surface treatment process for removal of the oxide layer is very much essential before plating the Mg alloy. Currently two processes such as

zinc immersion and direct electroless nickel plating are adopted to plate Mg alloys [1]. Etching in a solution of chromate and nitric acid followed by immersion in HF solution to form a conversion film is necessary for direct electroless nickel plating of Mg alloy [8].

Corrosion behaviour of electroless nickel coatings on Mg alloys was widely investigated [9-12]. By scanning through the available literature few studies were reported on electroless nickel ternary alloy coatings on the Mg alloy substrate. Zhang et al., studied the corrosion behaviour of electroless Ni-W-P and Ni-Sn-P alloys deposited on AZ91D substrate in 3 wt.% NaCl medium. They reported that these coatings showed 2 to 3 times improvement in the corrosion resistance as compared with plain Ni-P coatings [13, 14]. Further to enhance the corrosion resistance of Mg alloys, studies have been carried out by depositing multilayers [15] and duplex Ni-P coatings [16]. Vitry et al., reported that heat treatment carried out for NiP/NiB duplex coatings at 180°C for 4 h has improved both corrosion and wear resistance [17]. Changdong Gu et al., [15] have deposited the multilayer electroless nickel alloy system containing low (2 wt.%), high (9 wt.%) and medium (5.4 wt.%) P coatings over AZ91D Mg alloy to specifically prevent pitting corrosion. Chen Xiao-ming et al., investigated the corrosion behaviour of Ni-P/ Ni-W-P duplex coatings on AZ91D Mg alloy in 3.5% NaCl medium. They found that this system exhibited about one and five times improvement in the corrosion resistance as compared with plain Ni-P coating and bare substrate, respectively [16].

Another method of improving the corrosion resistance of electroless nickel alloys is by passivating the coated surfaces with Cr^{6+} and Cr^{3+} conversion films [18]. Potentiodynamic polarization studies carried out for these passive films indicated that the corrosion currents of these films are only about 1/25 of un-passivated coating.

To our knowledge detailed investigation on the electrochemical behavior of duplex coatings of Mg alloys using electrochemical impedance spectroscopy (EIS) has not been carried out. In the present manuscript we have made an attempt to prepare the electroless nickel alloy coatings using a

stabilizer-free bath. To further enhance the corrosion resistance, chromate passivation is also done over duplex coating as post treatment process.

In the present work, we have prepared plain Ni-P and duplex Ni-P/Ni-W-P coatings on AZ31B magnesium alloys using a stabilizer free carbonate bath. As a post treatment process, chromic acid passivation treatment is given for duplex coatings with and without heat treatment. Electrochemical evaluation of these coatings has been carried out using potentiodynamic polarization and EIS.

2. Experimental

AZ31B Magnesium alloy (2.5cm×2.5cm×0.2cm) was the substrate material. The chemical composition of the alloy is shown in the Table 1. The surface of the substrate material was wet-ground (using water) on 1000 SiC paper. The samples were washed with distilled water and dried. It was then subjected to various pretreatment steps and is given in Table 2. The initial weight and dimensions of the specimens were measured prior to pretreatment and pre-cleaning steps. Immediately after fluoride activation, the specimen was quickly transferred to the Ni-P coating bath placed in a constant temperature oil bath, to maintain the required temperature. After obtaining a required thickness of Ni-P coating, the sample was transferred to the Ni-W-P bath. The composition of the duplex (Ni-P and Ni-W-P) electroless nickel baths and plating conditions are given in Table 2. From the table it can be seen that plating baths were free from any stabilizers. The samples were coated for the required length of time, removed from the bath, washed with distilled water and air-dried. Final weight of the sample was determined and the coating rate in μm/hr was calculated from the weight gain. After plating, the samples were rinsed in distilled water and then were passivated immediately. After passivation, the samples were rinsed in running tap water followed by distilled water. Some of the AZ31B magnesium samples coated with Duplex Ni-P/NiWP were undergo heat treatments for 4 h at 150°C in an oven. These samples were also given the passivation treatment. Surface morphology and coating thickness of the untreated duplex (Ni-P/NiWP) and duplex passivated (duplex-P) coatings were characterized using Field Emission Scanning Electron with

Energy Dispersive X-ray Analysis (FESEM/EDAX model-Carl Zeiss Supra 40 VP). EDX analysis was used for the determination of phosphorus, tungsten, nickel and chromium on the surface and in the cross section of these coatings. Corrosion behaviour of all the coatings was studied by potentiodynamic polarization and electrochemical impedance spectroscopy measurements using CH instruments and the software used for fitting was Zsimp. A conventional three-electrode flat cell was used in which test sample was placed in a sample holder and the exposed surface area to the corrosive medium was approximately 1 cm^2. Platinum strip of 1 cm^2 area served as counter electrode and a standard calomel electrode (SCE) was used as the reference electrode. Prior to the beginning of the EIS measurements the sample was immersed in the corrosive medium (0.15M NaCl, pH 6.7) for about 10 min in order to establish the open circuit potential (E_{OCP}) or the steady state potential after which the impedance measurements were conducted using a frequency response analyzer (FRA). The spectrum was recorded in the frequency range of 10 mHz–100 kHz. The applied alternating potential had root-mean square amplitude of 10 mV on the E_{corr}. The impedance data was displayed as Nyquist and Bode plots. The Nyquist plot is a plot of real (Z') versus imaginary (Z'') impedance. At high frequency, the value of solution resistance (R_s) is obtained and at low frequency, the charge transfer resistance (R_{ct}) is deduced. The Bode plot is a plot of log|Z| vs log f and log f vs phase angle (θ), where |Z| is the absolute impedance and f is the frequency. The advantage of this plot is that the data for all the measured frequencies are shown and also a wide range of impedance values could be displayed. The frequency dependence of the phase angle indicates whether one or more time constants occur, which could be used to determine equivalent circuit parameters. After EIS measurements, the system was allowed to attain its stable open circuit potential. After reaching the stable open-circuit potential, the upper and the lower potential limits of linear sweep voltammetry were set at ± 200 mV with respect to the E_{OCP}. The sweep rate was 1 mV/s and the Tafel plot was obtained after the electrochemical measurements. The corrosion potential (E_{corr}), the corrosion

current density (i_{corr}) and polarization resistance (R_p) were deduced from the Tafel plot (that is, log i versus E plot). The corrosion current is obtained using the Stern-Geary equation [19]

3. Results and discussion

3.1 Surface Morphology (FESEM) and Composition Analysis (EDX)

In general electroless nickel deposits exhibit nodular morphology [20]. The extent of nodularity/ surface morphology depends on the characteristics of electroless nickel plating solution. It has been reported that the addition of small amount of inorganic additives to the bath improves the surface smoothness by reducing the growth of the nodules [21]. One of the present authors have found that the nodularity of the electroless nickel deposit is influenced by the anions used in the form of sulphates and chlorides. It was concluded that the presence of chloride anions results in smoother ternary NiWP deposits compared to the other anions. In the present study, all the coatings have been deposited over Mg alloy specimen and the as-deposited coatings were subjected to FESEM analysis to find out their surface morphology and are given in Fig. 1. It is evident that the plain NiP deposit exhibited nodular structure (Fig. 1(a)). It appears that these nodules are not continuous and the presence of pores is visible between these clusters of nodules. The size of these cluster nodules are of about 10 μm diameter (Fig. 1(b)). Nodularity has reduced to a great extent and coating appears smooth after NiWP deposited over plain NiP coating (Fig. 1(c)). Apart from that scattered bright particles (< 1 μm) are seen all over the surface (Fig. 1(d)). In the case of chromate passivated duplex coating, chromate passivation has resulted in the formation of slightly more no. of connected nodules compared to the duplex coating without any passivation treatment (Fig. 1(e)). Due to the presence of these wide nodules, the visibility of bright particles is much more compared to the duplex coated surface (Fig. 1(f)). These bright particles may correspond to the excess growth of nickel alloy over the nodules. The excess growth of nickel could be due to the mixed complex in the solution which acts as a direct precursor for the deposition of the alloy. Duplex coatings with passivation treatment have been heat treated below 200°C for 4 hrs for dehydration [22]. Surface images of these coatings

are given in Fig. 1 (g & h). These coatings exhibited coarse nodular morphology with scattered bright particles.

To find out the composition of these coatings EDX analysis has been carried out and the obtained results are given in Table 3. From the table it is evident that the plain NiP deposit contained about 6.5 wt.% P. It is surprising to notice that along with P and Ni elements the presence of Mg (4 wt.%) and F (5.4 wt.%) have also been detected during the composition analysis. As discussed in the above, plain NiP deposit exhibited nodular morphology with lot of porosity (Fig. 1(a)). It appears that formed pores are through pores connecting to Mg alloy surface. During the pretreatment, fluoride activation treatment has been followed for the specimen to deposit 10 μm thick binary NiP. Apart from this fluoride treatment, plating bath also contains ammonium fluoride as one of the ingredients. This could be the reason for the detection of both Mg and F elements during EDX analysis. Codeposition of W (2 wt.%) in NiP matrix has resulted in lower P content from 6.5 to 3.2 wt.%. Marginal variation in P and W contents are observed due to the heat treatment. Heat treated chromate passivated duplex coatings have exhibited almost same P and W contents as that of duplex coatings with an addition of about 0.18 wt.% Cr content. Metallographic cross-section of NiP/NiWP duplex coating has been prepared to find out the composition of the duplex coating. Spot EDX analysis has been carried out at a distance of 3 – 4 μm thicknesses. Cross-sectional images along with EDX line scan is shown in Fig. 2.

The coating thickness in Fig. 2a appears to be consistent with the measured values of about 25-30 μm as is evident from the line scan graph (Fig.2b). However, there is no clear demarcation between the Ni-P and the Ni-W-P layers in the duplex coating (Fig. 2c). Elemental composition obtained at 3 different regions of the cross-section is given in Table 4. The spot 1 EDX analysis carried out closer to the substrate surface showed about 6 wt.% P with traces of W which might be due to the inherent porosity of Ni-P coatings. Spot 2 analysis was done at a point roughly around the boundary of Ni-P/Ni-W-P coatings. The amount of P is slightly high (>6 wt%) with an increase in the amount of W

(1 wt.%). Spot 3 analysis was taken at a point further away from the substrate, presumably at the Ni-W-P coating region of the duplex coating. From the compositional analysis it is evident that (Table 4) there is a gradual decrease in P (2 wt.%) content and increase in the amount of W (1.3 wt.%) from the substrate/coating interface to surface of the duplex coating.

3.2 Corrosion characteristics of the coatings

In general, there are many methods available to evaluate the corrosion behavior of the coatings. Electrochemical impedance spectroscopy (EIS) and potentiodynamic polarization are the useful techniques to understand the corrosion behavior.

3.2.1 Potentiodynamic polarization

Potentiodynamic polarization curves obtained for bare, Ni-P, duplex, duplex-P and duplex-HTP coatings immersed in 0.15M NaCl solution are given in the Fig. 3. The corrosion parameters obtained from the plot are given in the Table 5. The potential obtained for the bare substrate is closer to the potential of Mg alloys reported for neutral aqueous solution (-1.5 V) [23]. From the table it can be seen that as-plated duplex and passivated duplex coatings showed positive potentials compared to other coatings. Whereas plain NiP coating exhibited higher corrosion current density (i_{corr}) value of about 218 $\mu A/cm^2$. It has been reported that medium P electroless NiP coatings exhibit i_{corr} value of about 25 $\mu A/cm^2$ when immersed in 3.5% NaCl solution. In the present study the higher i_{corr} value of NiP coating could be due to the porous nature of the coating (Fig. 1a). There is about 55 times decrease in the i_{corr} value in the case of as-plated duplex coating. It is clearly evident from the table that chromate passivated duplex coating exhibited lowest corrosion current densities in the range 0.5 – 1.8 $\mu A/cm^2$. Higher polarization resistance (Rp) value of about 61000 $\Omega\ cm^2$ has been obtained for duplex-HTP coating compared to other coatings indicating the better corrosion resistance of the coating.

3.2.2 EIS studies

Figure 4 shows the Nyquist plots obtained for the bare, Ni-P, as-plated duplex, duplex-P and duplex-HTP coatings in 0.15 M NaCl solution at their respective open circuit potentials in non-deaerated condition. The impedance parameters derived by fitting the data are given in the Table 6. Nyquist plot obtained for all the samples exhibited a two depressed semicircle showing two capacitive loops indicating the presence of two time constants. The semicircle of smaller diameter can be observed at the higher frequency region followed by the larger diameter semicircle at the intermediate and lower frequency regions. The semicircle obtained at higher frequency region is shown in in-set (Fig. 4 (c-e)) for as-plated duplex, duplex-P and duplex-HTP coatings. It is well known that the diameter of the semicircle is related with the corrosion resistance of the coating. Larger the diameter better is the corrosion resistance of the sample. Among the coatings, duplex-HTP coating showed larger semicircle as compared with other coatings indicating the improved corrosion resistance of the coating. From the table it can be seen that R_{ct} value obtained for this coating is about 34,630 Ω cm^2. The semicircle at the higher frequency region is related to the film/solution interface and the following semicircle at the intermediate and lower frequency regions is related to the coating/solution interface. At lower frequency region, inductive loops have been observed for the bare Mg alloy substrate and Ni-P coating. It has been reported that the inductance could arise due to the diffusion and adsorption of the electroactive species over the surface of the film and the substrate [24].

Figure 5 shows the Bode plots obtained for all the coatings developed. Absolute impedance vs frequency plot (log $|Z|$ vs log f) obtained for all the coatings is shown in Fig. 5a. The absolute value of impedance increases in the following order: Ni-P < bare < duplex < duplex-P < duplex-HTP. Apart from that it also exhibits more than one slope which indicates the presence of more than one or two time constants. Phase angle vs frequency (Fig. 5b) plot shows the phase angle of about 45° at the higher frequency region for all the coatings. The phase angle peaks varied from 20 to 60° at the intermediate frequency region and peaks distributed over the wide frequency range (10 kHz to

0.1 Hz). From the Fig. 5b it is evident that both bare substrate and Ni-P coating exhibited negative phase angle indicating the inductive behavior at the lower frequency region. In the case of duplex-HTP at lower frequency region, phase angle shifted closer to 40° due to its diffusion behavior.

The impedance spectra are fitted with the possible equivalent circuits shown in the Fig. 6 (a-e). Figure 6a shows the equivalent circuit used for fitting the EIS data obtained for bare Mg alloy showing two time constants in series with inductive elements. The circuit description code (CDC) for the equivalent circuit can be written as $R_s(Q_f(R_f(Q_{dl}R_{ct})(L_{ads1}R_{ads1})(L_{ads2}R_{ads2})))$ where R_s - solution resistance, R_f -film resistance, Q_f -film capacitance, R_{ct}-charge transfer resistance, Q_{dl} - double layer capacitance, L_{ads} -adsorption inductance, R_{ads}- adsorption resistance. Constant phase element (CPE) accounts for the deviation from ideal capacitive behavior and is related to surface inhomogeneities [25]. The capacitance is replaced with CPE for better quality fit. Q stands for constant phase element. This element can be written in admittance form as:

$Y(\omega) = Y_0(j\,\omega)n$

Where Y_0 and 'n' are the adjustable parameters used in the non-linear least-square fitting. Here, 'n' value always lies in between 0.5 and 1.

Mansfeld et al., [26] have reported the occurrence of depressed capacitive loop followed by inductive loop for AZ31 Mg alloy in 0.5 N NaCl. Similarly Song et al., [27] have also observed the presence of capacitive loop followed by the inductive loop in NaCl medium for AZ91 Mg alloy. In this study the similar impedance spectra was observed for bare Mg alloy showing capacitive and inductive loops over the investigated frequency range which could be due to the adsorption of electroactive species such as Mg^{+}, Mg^{+2}, OH^{-} and Cl^{-} over the surface.

Figure 6b shows the equivalent circuit used for fitting the data of the Ni-P coating on exposure to corrosive medium. In this case, coating capacitance (Q_{coat}) and coating resistance (R_{coat}) are observed in parallel with charge transfer resistance and double layer capacitance. They are in series with adsorption inductance and resistance respectively. The circuit description code can be written

as $R_s(Q_{coat}(R_{coat}(Q_{dl}R_{ct})(L_{ads1}R_{ads1})))$. The R_f and Q_f are the resistance and capacitance of the dissolved film formed at the solution/ film interface and R_{ct} and Q_{dl} are related with the coating electrolyte interface. The porous Ni-P coating allows the electrolyte to easily reach the substrate that leads to the dissolution and adsorption of electroactive species over the substrate resulted in the formation of L_{ads} and R_{ads} respectively. Compositional analysis carried out for these coatings it is evident that Ni-P coatings showed the presence of Mg and F with traces of O and Cr which have resulted during the initial pretreatment process of the substrate. Due to this porosity, corrosive species can easily penetrate and attack the substrate. This resulted in the inductive behavior at the lower frequency region which is the characteristic of the substrate. The total resistance obtained for Ni-P coatings is very low of about 206 Ω cm^2 when compared with the substrate (Table 5).

The equivalent circuit shown in the Fig. 6c is used for fitting the data obtained for duplex and duplex-P coatings respectively showing three time constants. However, in the Nyquist plot (Fig. 4c) the presence of three capacitive loops is not easily distinguishable due to the overlapping. First, second and third time constants are related with the film resistance and capacitance, coating resistance and capacitance and R_{ct} and Q_{dl} respectively. The CDC for these coatings can be written as $R_s((Q_{film}R_{film})(Q_{coat}R_{coat})\ (Q_{dl}R_{ct}))$. It is well known that electroless Ni-P coating in the presence of corrosive medium undergoes dissolution (Ni) which results in the enrichment of P over the surface and forms a protective hypophosphite layer [28]. In the case of duplex coatings, R_{film} and Q_{film} arise due to the dissolution of nickel from Ni-W-P layer. Other two time constants arise due to the resistance offered by the coating and the relative electron transfer taking place near the electrode/ electrolyte interface. The coating resistance and charge transfer resistance of the coatings are about 2488 and 2996 Ω cm^2. From the table it is evident that the total resistance offered by the duplex coating is 28 times higher when compared with Ni-P coating. From the above it is clear that Ni-P coating obtained in this study is porous and non-protective in nature, however, the dense Ni-W-P coating acts as a barrier layer and showed improved corrosion resistance. In the case of duplex-P

coatings, even though the resistance offered by the film is almost similar to the duplex coating, there is about 3 times increase in the total resistance of the coating. It could be due to the combination of both passive chromate film and enriched P layer over the passivated duplex coating. In general, chromate passivation leads to the formation of $(Cr^{3+}\text{-}O\text{-}Cr^{+6})_n$ polymeric network on the coating surface. Hence, the passivated layer imparts additional resistance to the coating.

The equivalent circuit obtained for duplex-HTP coatings (Fig. 6e) shows the parameters such as Q_{film}, R_{film}, Q_{coat}, R_{coat} and W (Warburg impedance) respectively. The CDC can be written as $R_s(Q_{film}(R_{film}(Q_{coat}(R_{coat}W))))$. In general, W is the infinite length diffusion element occurring at the lower frequency region which is the combination of diffusion resistor and capacitor. It provides the additional resistance to the coating by preventing the entry of the electrolyte through the coating due to the presence of oxide or corrosion products. From the surface images of duplex-HTP it is evident that (Fig. 1g) the surface appears non-uniform nodular morphology. Further passivation treatment imparted additional resistance to the coating leading to Warburg impedance. Similar kind of circuit was used for chromate conversion coated on Alclad 2024 aluminum alloy exposed to 3% NaCl medium [29]. Q_f and Q_{coat} values obtained for heat treated passivated samples were very low compared to other coatings. The n_f values for both passivated coatings were about 0.41 and 0.64 respectively indicating the diffusion behavior. The duplex-HTP samples showed the Warburg diffusion of about 3.767×10^{-4} cm^{-2} $\sqrt{s}$ Ω^{-1}. The n_{dl} values obtained for all the coatings were closer to 1 indicting the pure capacitive behavior. Q_{dl} value obtained for duplex coatings were higher 720.6 $\mu F/cm^2$ as compared with other coatings indicating the lower capacitance behavior.

4. Conclusions

Electroless duplex Ni-P/Ni-W-P coatings were successfully developed on AZ31B magnesium alloy using stabilizer-free nickel carbonate bath. Ni-P coating exhibited nodular morphology with porosity. Duplex Ni-P/Ni-W-P coating exhibited less nodular, dense and smooth appearance.

From the compositional analysis it was found that Ni-P and duplex coatings showed the presence of 6 and 3 wt.% P respectively. About 2 wt.% tungsten was incorporated in the ternary Ni-W-P coating. Potentiodynamic polarisation data showed lower corrosion current density of 0.547 $\mu A/cm^2$ for duplex-HTP coating which was about 8 and 430 times lower than duplex and Ni-P coatings, respectively. Higher total resistance values obtained from EIS studies indicated the improved corrosion resistance of the duplex-HTP coating. Nyquist plot obtained for bare substrate and Ni-P showed the presence of inductance behaviour at the lower frequency region due to the adsorption of the electroactive species over the substrate though the porous oxide layer. In the case of duplex passivated and HTP coatings exhibited only capacitive behaviour.

Acknowledgements

The authors thank the Director, CSIR-NAL for giving permission to publish this work. Help received from Mr. M. Ganesh to prepare the samples is acknowledged. The authors also thank Mr. Siju for FESEM work.

References

[1] J. E. Gray, B. Luan, J. Alloy compd. 336 (2002) 88.

[2] X.B. Chen, H.Y. Yang, T.B. Abbott, M.A. Easton, and N. Birbilis, Corrosion, 68 (2012) 518

[3] C. S. Lin, S. K. Fang, J. Electrochem. Soc. 152 (2005) B54.

[4] G. Reiners, M. Griepentrog, Surf. Coat. Technol. 76 (1995) 809.

[5] P.L. Hagans, C.M. Haas, Chromate conversion coatings, in: ASM Handbook, Surface Engineering, 5, ASM International, 1994, pp.104

[6] J. N. Balaraju, K.S. Rajam, Surf. Coat. Technol. 195 (2005) 154.

[7] J. N. Balaraju, V. Ezhil Selvi, V.K. William Grips, K.S. Rajam, Electrochim. Acta, 52 (2006) 1064.

[8] X. S. Li, W. X Zhang, Z. H. Jiang, Trans. Nonferrous Met. Soc. China 17 (2007) s835.

[9] Hongwei Huo, Ying Li, Fuhui Wang, Corros. Sci. 46 (2004) 1467.

[10] Shiyan Zhang, Qing Li, Xiaokui Yang, Xiankang Zhong, Yan Dai, Fei Luo, Mater. Charact. 61 (2010) 269.

[11] D. Seifzadeh, Z. Rajabalizadeh, Surf. Coat. Technol. 218 (2013) 119.

[12] Jianzhong Li, Yanwen Tian, Zhenqi Huang, Xin Zhang, Appl. Surf. Sci. 252 (2006), 2839.

[13] W.X. Zhang, N. Huang, J.G. He, Z.H. Jiang, Q. Jiang, J.S. Lian, App. Surf. Sci. 253, (2007), 5116.

[14] W. X. Zhang, Z. H.Li, G. Y. Jiang, J. S. Lian, Surf. Coat. Technol. 202,(2008),2570

[15] C. Gu, J. Lian, Z. Jiang, Adv. Eng. Mater. 7 (2005) 1032.

[16] Chen Xiao-ming, G. Y . Li, J. S. Lian, Trans. Nonferrous Met. Soc. China 18 (2008) s323.

[17] V. Vitry, A. Sens, A.-F. Kanta, F. Delaunois, , Surf. Coat. Technol. 206 (2012) 3421

[18] Songlin Mu, Ning Li, Deyu Li, Zhongli Zou, Electrochim . Acta, 54 (2009) 6718.

[19] M. Stern, A. L. Geary, J. Electrochem. Soc. 104 (1957) 56.

[20] G.O. Mallory, J.P. Hajdu, Electroless Plating, AESF, USA, 1990.

[21] Linda L. Zhong, Connie C. Liu, J.D. John St., Jeff D., U.S. Pat. US6410104.

[22] J. W. Zhang, L.-F. Hou, B. –S. Xu., Trans. Mater. Heat Treat. 31 (2010) 137.

[23] Guang-Ling Song (Eds). Corrosion of magnesium alloys,2011,Woodhead publication.

[24] I.V. Aoki, M.C. Bernard, S.I. Cordoba de Torresi, C.Deslouis, H.G. de Melo, S. Joiret, B. Tribollet, *Electrochim. Acta* 46 (2001) 1871

[25] J.R. Macdonald, Impedance Spectroscopy-Emphasizing Solid Materials and System, John Wiley & Sons, 1987, p. 17

[26] F. Mansfeld, C. H. Tsai, H. Shih, Computer modelling in corrosion, ASTM STP 1154, R. S. Munn, Ed., American Society for Testing and Materials, Philadelphia, 1992, 186

[27] Y. W. Song, D.Y.Shan, R. S. Chen, E.-H. Han, Corr. Eng. Sci. Technol. 46, 2011, 719

[28] J. N. Balaraju, K.S. Rajam, Surf and Coat Technol, 195(2005) 154.

[29] P. Campestrini, E. P. M van Westing, J. H. W. de Wit, Electrochim Acta, 46 (2001) 2631

Figure Captions

Fig.1 FE-SEM images of as-deposited samples AZ31B Mg samples at 1000X and 10,000Xmagnifications: (a and b) Ni-P, (c and d) Ni-P/Ni-W-P (e and f) passivated Ni-P/Ni-W-P and (g and h) Heat treated passivated Ni-P/Ni-W-P

Fig.2 (a) Cross sectional FE-SEM micrograph (b) EDX line spectrum of Ni-P/Ni-W-P coatings and (c) EDX spot analysis throughout the coating.

Fig.3 Potentiodynamic polarization curves obtained for (a) Ni-P, (b) Duplex Ni-P/Ni-W-P, (c) passivated Duplex Ni-P/Ni-W-P, and (d) heat treated passivated Duplex Ni-P/Ni-W-P. Also shown are the polarization curves of bare Mg alloy substrate.

Fig. 4 Nyquist plots obtained for: (a) bare Mg alloy (b) Ni-P, (c) Duplex Ni-P/Ni-W-P, (d) passivated Duplex Ni-P/Ni-W-P, and (e) heat treated passivated Duplex Ni-P/Ni-W-P.

Fig.5 Bode plots (a) log $|Z|$ vs. log f and (b) phase angle vs. log f for : (●)Bare Mg alloy, (◆) Ni-P, (▲) Duplex Ni-P/Ni-W-P, (★) passivated Duplex Ni-P/Ni-W-P, (*) heat treated passivated Duplex Ni-P/Ni-W-P

Fig.6 Equivalent circuits used for fitting the electrochemical data of : (a)bare AZ31B Mg , (b) Ni-P, (c) Duplex Ni-P/Ni-W-P and passivated Duplex Ni-P/Ni-W-P and (d) heat treated passivated Duplex Ni-P/Ni-W-P

Table 1 Chemical composition (in wt%) of AZ31B Mg alloy

Al	Zn	Mn	Si	Cu	Ni	Fe	V	O	Mg
2.745	0.940	0.215	0.055	0.001	0.001	0.005	0.003	2.140	
Balance									

Table 2 Composition and operating conditions of the Duplex Ni-P/Ni-W-P coating on AZ31B Mg alloy

Operation	Plating bath composition		Conditions
Ultrasonic cleaning	Acetone		10 min
Alkaline cleaning	NaOH $Na_3PO_4.12H_2O$	45 g/l 10 g/l	65˚C 15-20 min
Acid etching (pickling)	CrO_3 g/l HNO_3(69% V/V) ml/l	125 100	Room temperature 40s
Fluoride activation	HF(40%) ml/l	125	Room temperature 1-2 min
Ni-P plating	$NiCO_3$ HF(48%) Citric acid NH_4HF_2 $Na_2H_2PO_2.H_2O$ $NH_3.H_2O$ ml/l	10 g/l 9 ml/l 5 ml/l 10 ml/l 20 g/l 30	pH 7.1 80-82 ˚C Mild magnetic stirring
Ni-W-P plating	$NiCO_3$ HF(48%) Citric acid $Na_2H_2PO_2.H_2O$ NH_4HF_2 Na_2WO_4 $NH_3.H_2O$	10 g/l 30 g/l 5 ml/l 20 g/l 10 g/l 12 g/l 30 g/l	pH 7 82±2˚C 2 hrs Mild magnetic stirring
Passivation	CrO_3 $K_2Cr_2O_7$	2.5 g/l 120 g/l	90-100˚C 10 min

Table 3 EDAX data of the as deposited samples

Elements	Composition in wt%		
	Spot 1	Spot 2	Spot 3
P	5.85	6.37	1.84
W	0.42	0.89	1.27
Ni	93.74	92.47	85.1

(HTP)-Heat treated passivated (P)- Passivated

Table 4 EDX data obtained on the duplex sample at different spots

Samples	Elements in wt %					
	P	W	Cr	Mg	F	Ni
Ni-P	6.56	-	-	4.22	5.42	82.75
Duplex Ni-P/Ni-W-P	3.23	2.03	-	-	-	94.70
Duplex Ni-P/Ni-W-P-(P)	3.46	2.30	0.18	-	-	91.26
Duplex Ni-P/Ni-W-P-(HTP)	3.30	2.12	0.19	-	-	91.28

Table 5 Potentiodynamic polarization data of Ni-P, duplex Ni-P/Ni-W-P coatings on AZ31B Mg alloy in 0.15 M NaCl solution

Samples	E_{corr} (V)	i_{corr} (μ A/cm^2)	R_p (Ω cm^2)
AZ31B	-1.54	8.23	548
Ni-P	-1.16	218.7	135
Ni-P/Ni-W-P	-0.44	4.304	3996
Ni-P/Ni-W-P (P)	-0.787	1.857	19351
Ni-P/Ni-W-P (HTP)	-0.673	0.547	61076

(HTP)-Heat treated passivated (P)- Passivated

Table 6 EIS data obtained by equivalent circuit simulation of the different coatings studied in the present work

Samples	Q_f-Y_0 (μF/cm^2)	n_f	R_f (Ω-cm^2)	Q_{coat}-Y_0 (μF/cm^2)	n_{coat}	R_{coat} (Ω-cm^2)	Q_{dl}-Y_0 (μF/cm^2)	n_{dl}	Rct (Ω-cm^2)	L_{ads-1}	R_{ads-1} (Ω-cm^2)	
Bare	0.873	0.88	83.30	-	-	-	5.930	0.94	650.8	161.0	280.0	
Ni-P				0.031	0.98	65.40	58.42	0.91	129.0	37.2	12.1	
Ni-P/Ni-W-P	112.0	0.85	54.0	0.029	0.98	2488.0	720.6	0.80	2996.0	-	-	
Ni-P/Ni-W-P (P)	0.029	0.98	54.00	70.3	0.41	5039	36.69	0.91	18050	-	-	
Ni-P/Ni-W-P(HTP)	0.0001	0.64	60.78	0.0260	0.98	34570				-	-	

(HTP) -Heat treated Passivated (P) - Passivated

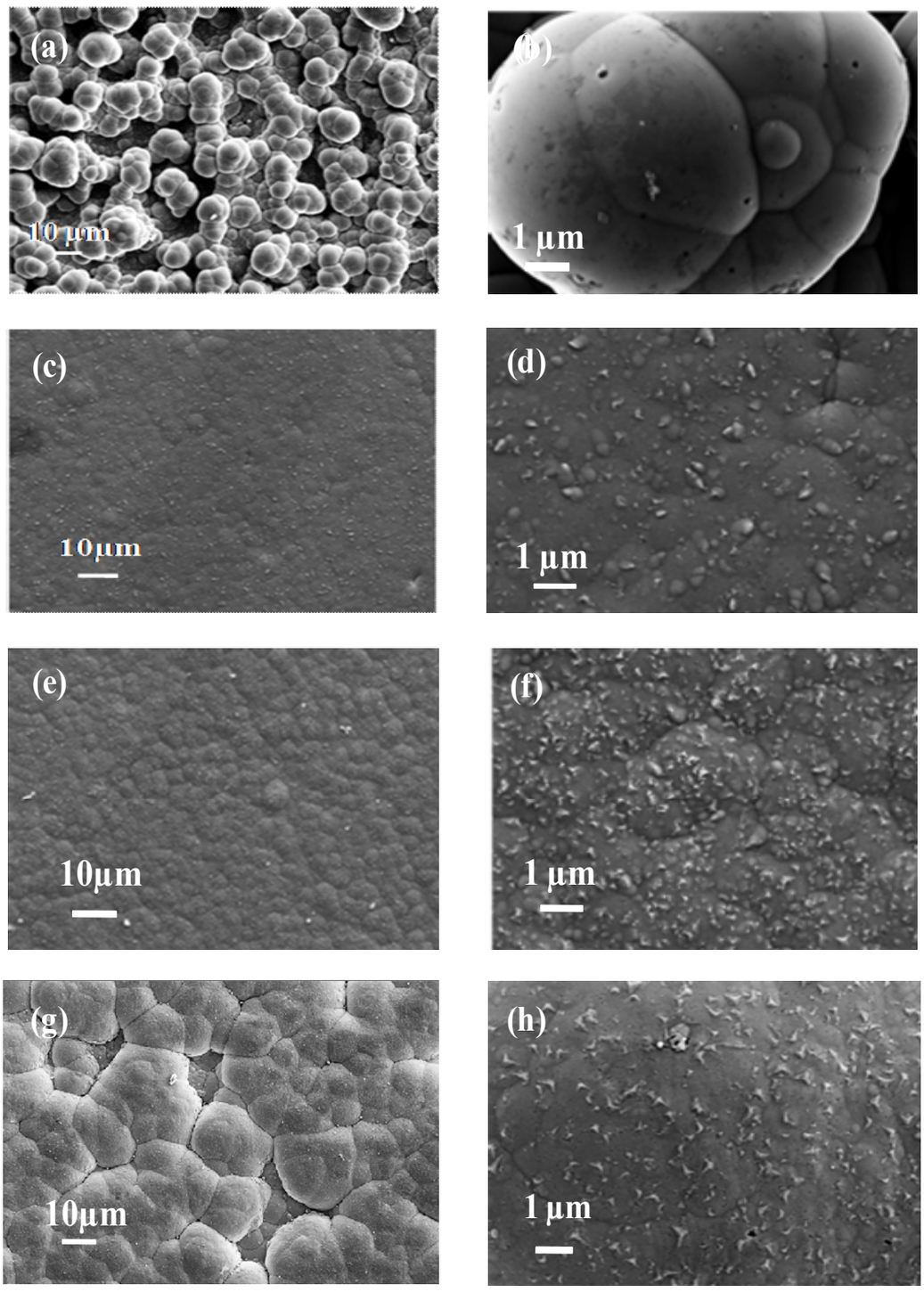

Fig. 1

(a)

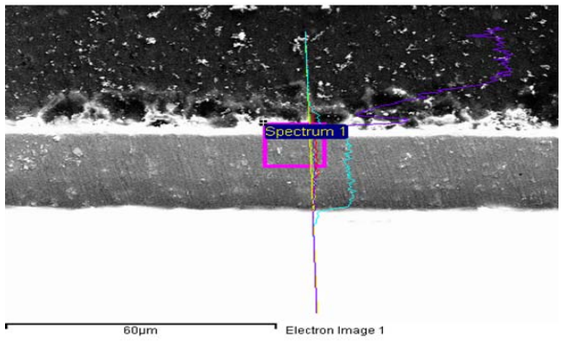
Spectrum 1
60µm
Electron Image 1

(b)

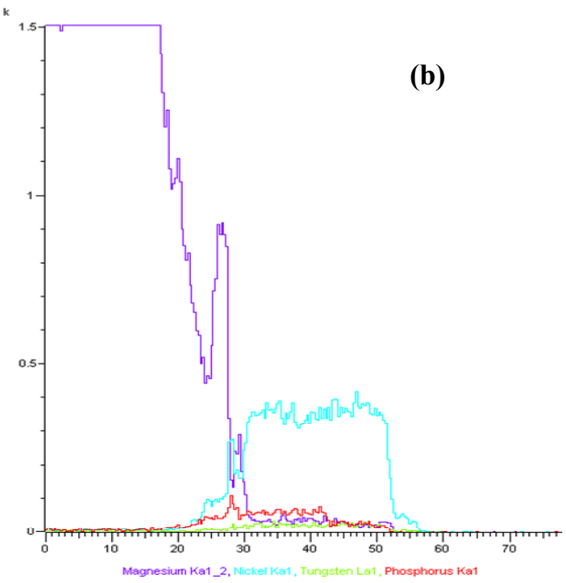
k
1.5
1
0.5
0
0
10
20
30
40
50
60
70
Magnesium Ka1_2, Nickel Ka1, Tungsten La1, Phosphorus Ka1

(c)

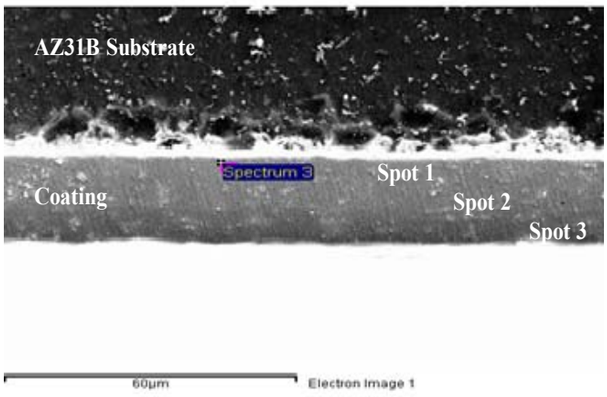
AZ31B Substrate
Spectrum 3
Spot 1
Coating
Spot 2
Spot 3
60µm
Electron Image 1

Fig.2

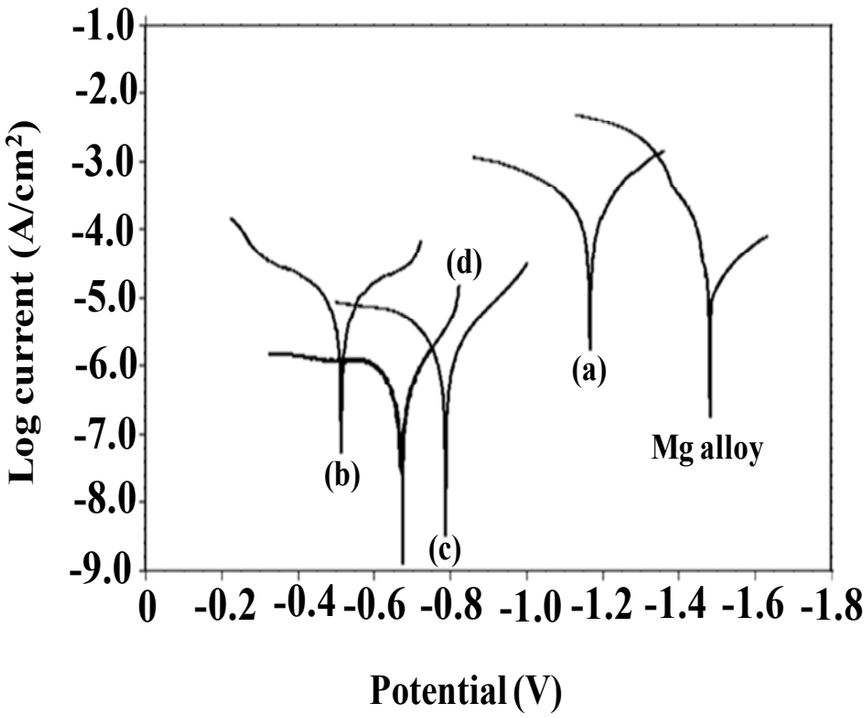
-1.0
-2.0
-3.0
-4.0
-5.0
-6.0
-7.0
-8.0
-9.0
Log current (A/cm²)
0
-0.2
-0.4
-0.6
-0.8
-1.0
-1.2
-1.4
-1.6
-1.8
Potential (V)
(a)
(b)
(c)
(d)
Mg alloy

Fig. 3

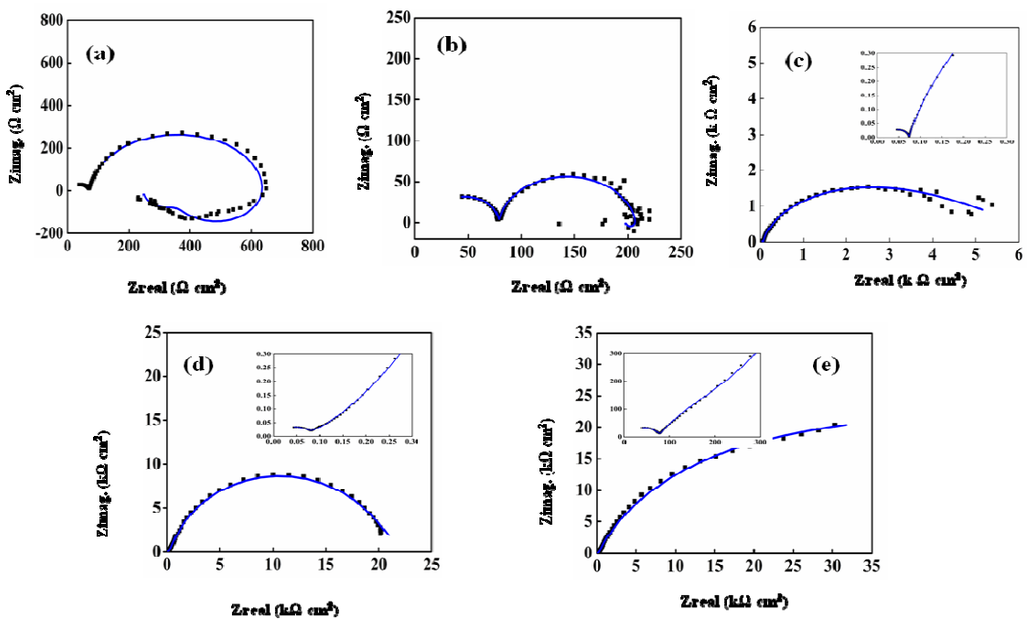
(a)
Zimag. (Ω cm²)
Zreal (Ω cm²)
(b)
Zimag. (Ω cm²)
Zreal (Ω cm²)
(c)
Zimag. (k Ω cm²)
Zreal (k Ω cm²)
(d)
Zimag. (kΩ cm²)
Zreal (kΩ cm²)
(e)
Zimag. (kΩ cm²)
Zreal (kΩ cm²)

Fig. 4

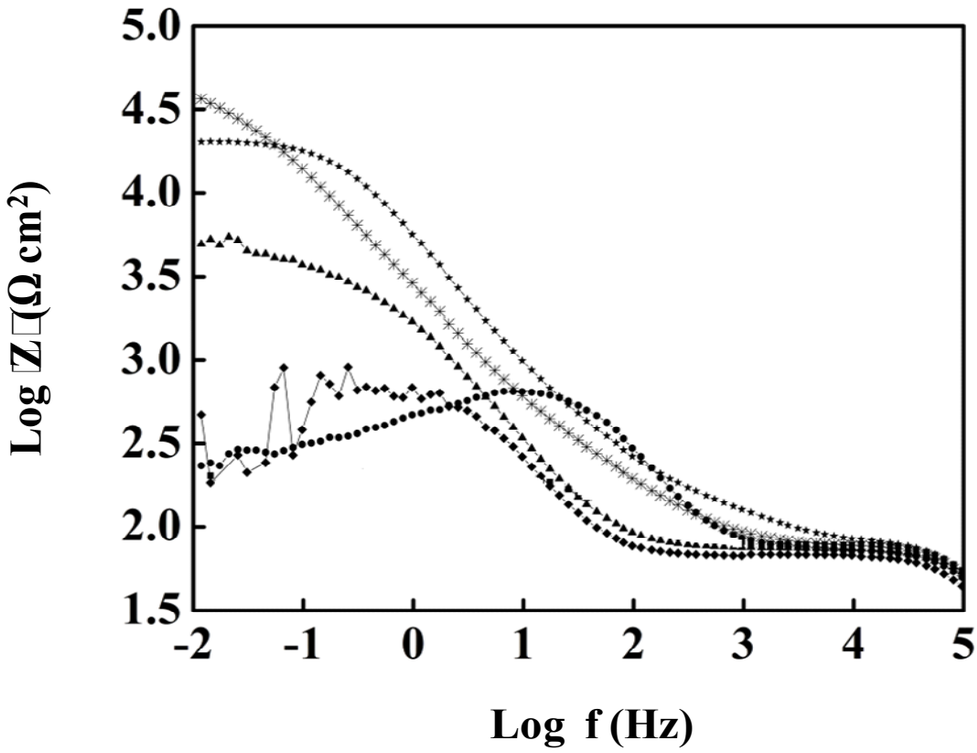

Fig.5a

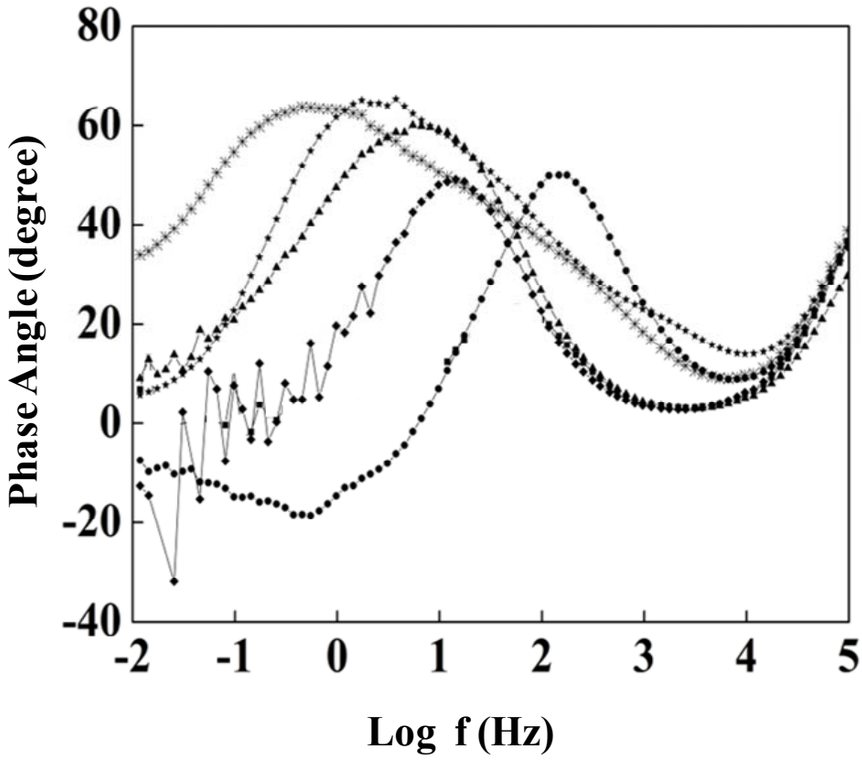

Fig. 5(b)

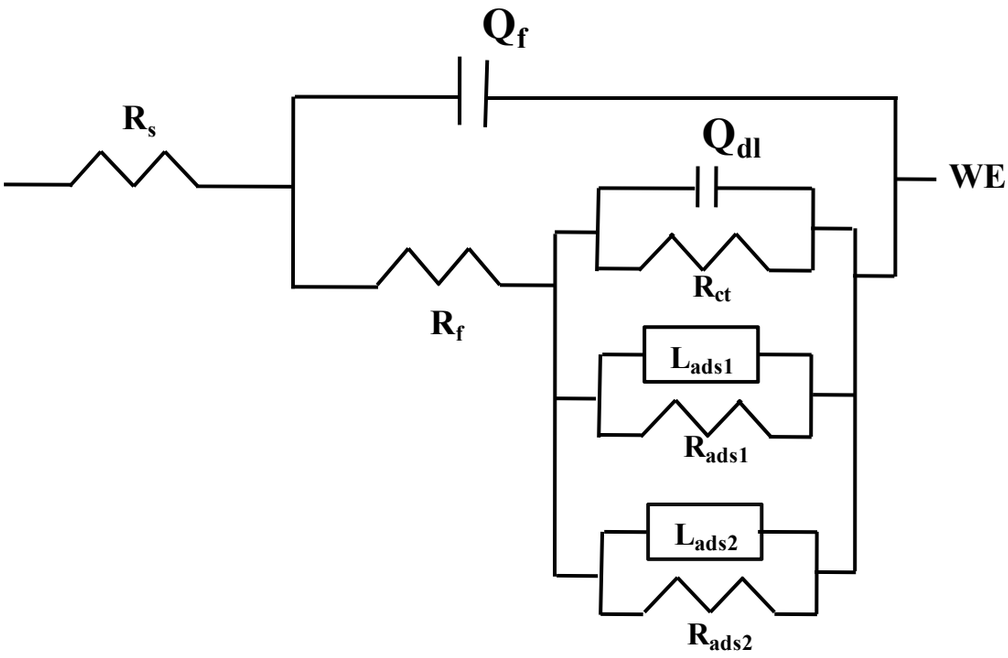

Fig.6a

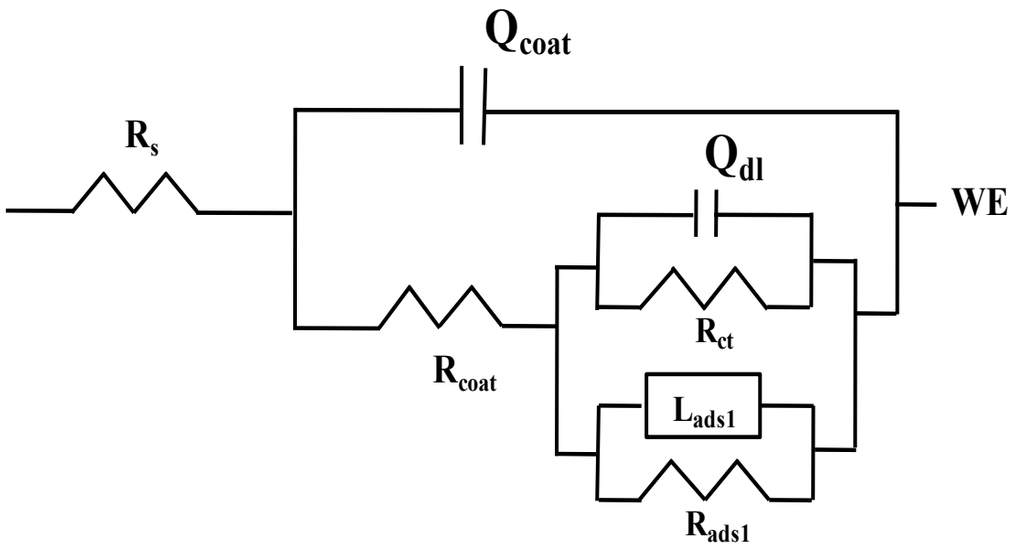

Fig.6b

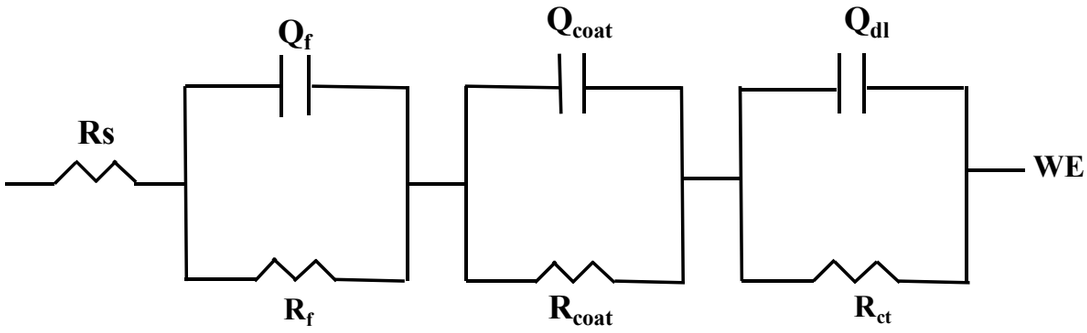

Fig. 6c

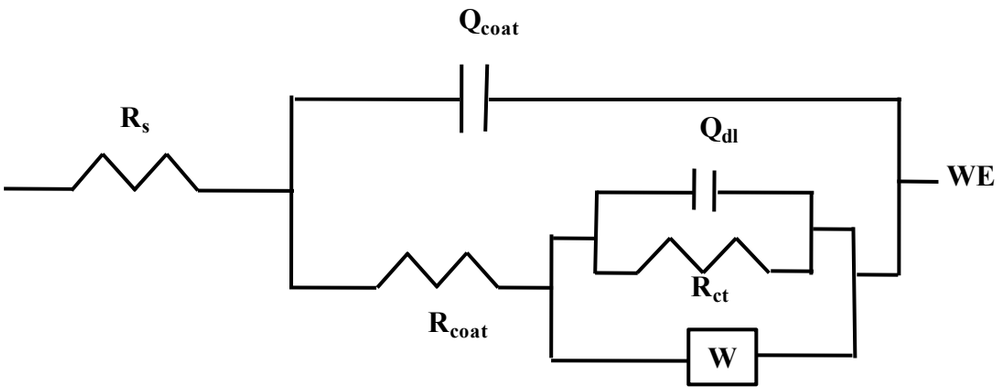

Fig. 6d